Available online at www.sciencedirect.com

ScienceDirect

Procedia Engineering 109 (2015) 181 – 188

Procedia Engineering

www.elsevier.com/locate/procedia

XXIII Italian Group of Fracture Meeting, IGFXXIII

# Experimental and numerical investigation on shear propagation of subsurface cracks under rolling contact fatigue

Giorgio Donzella, Angelo Mazzù*, Candida Petrogalli

University of Brescia, Department of Mechanical and Industrial Engineering, via Branze, 38, 25123, Brescia, Italy

**Abstract**

Shear propagation of subsurface cracks under rolling contact fatigue was investigated on quenched and tempered SAE 5135 gear steel. The formation of subsurface cracks almost parallel to the contact surface was observed, highlighting the de-attachment of micro-particles from the cracks surfaces due to shear. Subsequent wear and plasticization processes lead to fragmentation of these particles, which transform in a smaller incoherent structure, and to the formation of a gap between the crack faces. The gap is maximum in the central part of the crack, with a dimension of some microns, whereas it tends to zero approaching the crack tips. Moreover, wear reduces the roughness of the crack faces by smoothing the asperities.

A FEM model was developed to simulate the process of crack propagation in presence of asperities along the crack path, by taking in to account their shape variation due to wear. For this aim, the crack was divided in several zones, assigning different faces roughness to each of them according to the experimental evidence. The significant influence of the roughness severity in determining the crack driving force could be quantified by this model, putting in evidence its locking effect for varying crack length.



Peer-review under responsibility of the Gruppo Italiano Frattura (IGF)

*Keywords:* Rolling contact fatigue; shear propagation; subsurface cracks

## 1. Introduction

Subsurface crack nucleation and propagation is a typical damage mechanism occurring under rolling contact fatigue of hard materials. It can lead to significant failures consisting in the de-attachment of surface layers: these failure phenomena are called in different ways, such as spalling, shelling, case crushing [1-2]. In hard materials, crack

* Corresponding author.
*E-mail address:* angelo.mazzu@unibs.it



Peer-review under responsibility of the Gruppo Italiano Frattura (IGF)
doi:10.1016/j.proeng.2015.06.230

nucleation is strongly favored by microstructural in-homogeneities such as inclusions (typically oxides and sulphides) [3-5].

Once a subsurface crack has nucleated, it can propagate for a long way before branching towards the surface, thus determining the sudden de-attachment of large portions of material with a consequent catastrophic and unexpected failure.

It is therefore of particular importance to deeply understand how and under which circumstances subsurface cracks initiate and grow. While the onset of subsurface cracks in a hard steel (for gears construction), in relationship with inclusion content, was treated in a previous paper [6], their propagation is here analyzed with particular attention to the effect of shear stresses on the material layers close to the crack faces. In fact, it has been recognized that in a rolling contact fatigue process subsurface cracks mainly propagate in mode II and mode III, often in a direction parallel to the contact surface [7-9].

A very few studies have been carried out up to now to analyze and characterize this type of crack propagation in terms of mechanism, crack growth threshold and rate, because of the difficulty in reproducing this phenomenon in laboratory specimens. The main reason of this difficulty is that shear propagation is an unstable process, usually early changing into mode I; the reason why subsurface cracks proceed by shear also for a long way under rolling contact fatigue has been explained by the presence of an important compressive T stress which prevents mode I branching. Following this hypothesis, shear tests procedures in presence of an imposed compressive stress parallel to the crack faces have been developed by some researchers [10-11].

In the present paper, a contribution to the understanding of these topics is given, by analyzing in detail an actual subsurface crack generated by rolling contact tests on a ring specimen made of a gear steel. Optical and electron microscope observations allowed describing different phases by which subsurface cracks grow. In particular, the role of shear stresses in determining the fragmentation of material layers near the crack faces, consequent debris generation and gap formation between crack faces is clearly shown. These evidences justify the "short crack" behaviour in shear mode, which has been recently put in evidence by other researchers by means of torsion tests [11-12]. It has been highlighted in particular that the closure effect due to friction and locking mechanism between crack faces asperities during sliding can greatly increase the crack growth threshold [11]. A FEM model was also developed to simulate the crack propagation, taking in to account the locking effect of asperities between the crack faces and its variation with the crack length, thus providing a quantitative assessment of this mechanism.

## 2. Experimental investigation of the subsurface crack

The experimental investigation refers to a ring specimen in hardened and tempered SAE 5135 steel used for gear production. It was one of a series of specimens previously tested under Rolling Contact Fatigue (RCF) in pure rolling condition with water lubrication, using a bi-disk machine [6]. The rings inner and outer diameters are respectively 148 mm and 175 mm, while their thickness is 10 mm. They were tested against counteracting disks with 65 mm diameter, made of quenched and tempered 100Cr6 steel (hardness 60 HRC), as shown in the scheme of Fig.1. RCF tests were carried out up to the occurrence of severe damage phenomena, which always appeared as suddenly occurring macro-spalling, without premonitory damage signs on the contact surface. This fact induced to consider the spalling phenomenon as originated beneath the rolling track, due to the nucleation and propagation of subsurface cracks. This result agrees with the experimental evidences observed by Cheng et al. [10] on a bearing steel.

The specimen under investigation was tested at a nominal contact pressure of 2000 MPa for $8.17\times10^5$ cycles, after which the macro-spalling occurred. The ring was then cut along its transversal section (see Fig.1) and observed by optical and electron microscope, analyzing the material layer beneath the surface in zones different from that interested by the macro-spalling. In particular, subsurface cracks not yet developed into spalling were searched, in order to study the damage mechanism in the intermediate stage.

In Fig.2, a significant subsurface crack found in the transversal section is visible. Its orientation, approximately parallel to the contact surface, indicates a preeminent mode II propagation. Examining more in details some zones of this crack, a local "zigzag" propagation can be seen. Moreover, it can be observed that the crack gradually opens from the tip to the central part, with the maximum gap of the order of a few microns, and that several micro-particles are entrapped between the crack faces acting as "third bodies".

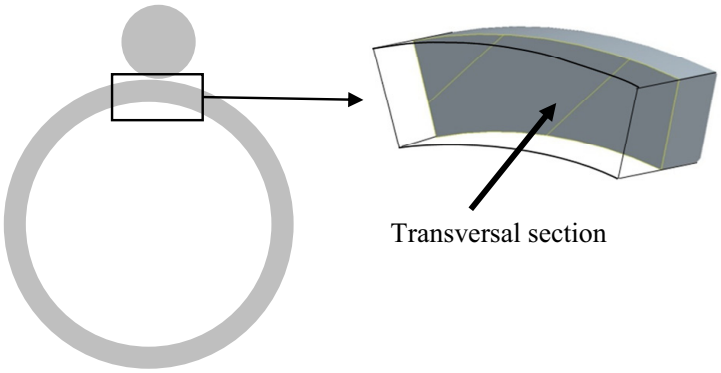


Fig. 1. Definition of specimen section

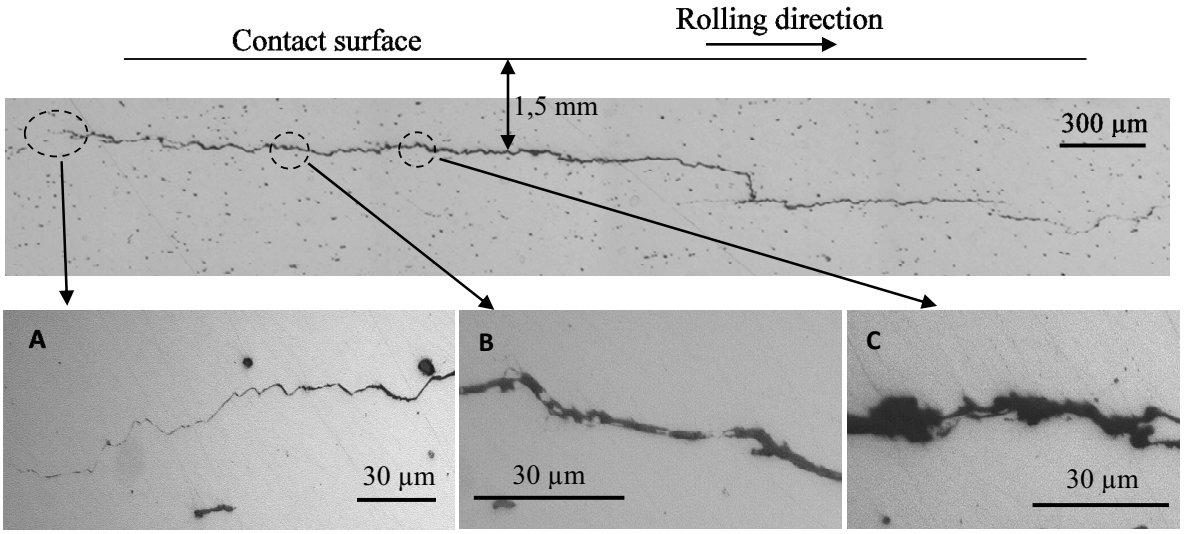


Fig. 2. Subsurface crack, with details of different zones

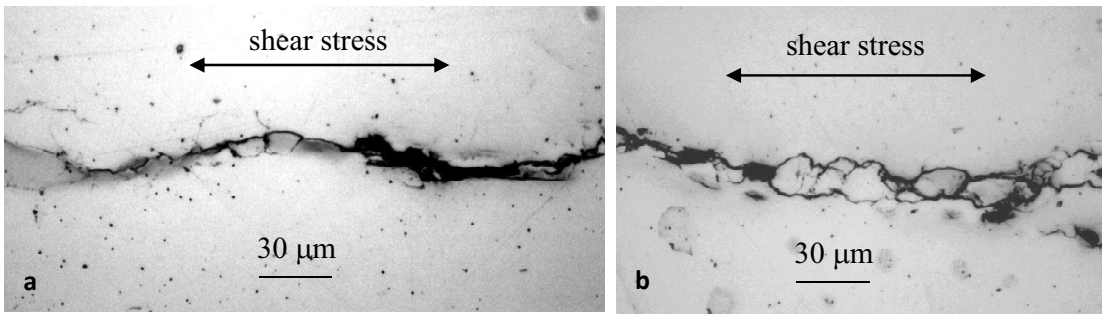


Fig. 3. Details of a crack

The formation of these micro-particles can be appreciated by the picture reported in Fig.3a, which shows the typical wave aspect of the crack and the incipient de-attachment of the micro-particles from the crack faces. In Fig.3b, this phenomenon is more advanced, showing the almost complete de-attachment of several micro-particles. These evidences can be imputed to the action of alternating shear stress with a concomitant compressive normal stress due to the contact force, which induces wear of the cracks faces, here appreciable at its initial stage. In some zones, several micro-particles are further fragmented and plasticized, generating a finer microstructure appearing as a grey band between the crack faces, as shown in Fig.4. A similar evidence was found by Matsunaga et al. in torsion tests [11].

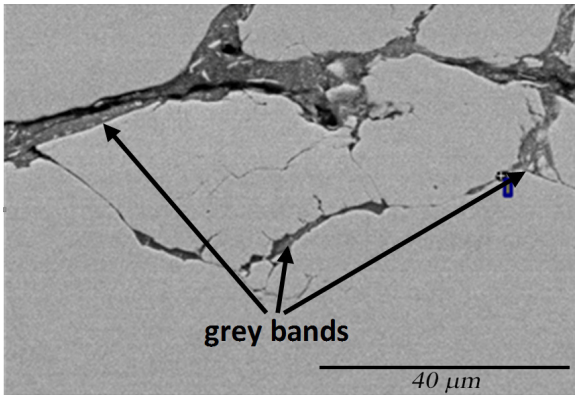


Fig. 4. Details of fine structure generated by the fragmentation of microparticles.

Thus, moving from the crack tip to the central zone, the evolution of the interaction mechanisms between the crack faces can be observed and synthesized in the following stages:

- Crack faces sliding due to shear stresses with concomitant compressive normal stress, which determines micro-failures of the contacting material layers;
- Consequent formation of micro-particles acting as third bodies in the wear phenomenon between crack faces;
- Fragmentation of micro-particles into a finer microstructure;

It has also to be observed that wear of contact surface asperities reduces their slope: a correspondent reduction of the locking effect between crack faces is therefore expected as well.

The specimen was finally broken after immersion in liquid nitrogen, in order to put in evidence the surface of the observed crack. Fig. 5 shows some details of the fracture surface, highlighting in particular the presence of evident sliding and flaking phenomena, typical of shear propagation (a), and the fine structure generated by the fragmentation of micro-particles (b).

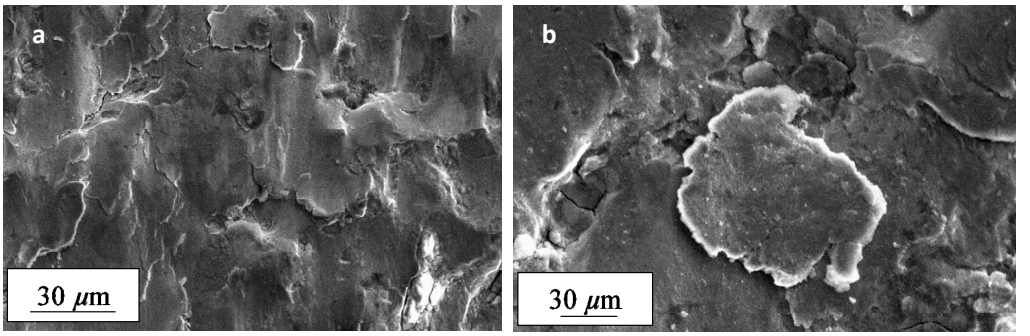


Fig. 5. Detail of fracture surface, showing shearing and flaking

## 3. Simulation of subsurface crack propagation

The mechanism of subsurface crack propagation was analyzed by means of Finite Element analyses using the ABAQUS 6.5 code, taking the crack shown in Fig. 2 as reference case. The material model for the SAE 5135 steel was linear elastic with Young modulus $E$=206 GPa and Poisson coefficient $\nu$=0.3. The action of the counteracting roller in 100Cr6 steel was simulated by means of a Hertz load distribution passing along the contact, with the same value as in the experimental tests. A subsurface crack at 1.5 mm depth below the contact surface was modeled by 2D plane strain elements; the quarter point technique was used for modeling the crack tips. Unilateral contact was imposed between the crack faces, with 0.25 Coulomb friction coefficient, as a reasonable value for steel smooth surfaces. The crack front was modeled with a serrate pattern, with teeth of different geometry for simulating the different roughness typology observed along the experimental crack front. In Fig. 6 the mesh of the crack front is shown. The pitch $p$ and the slope $\vartheta$ define the teeth geometry, whereas $a$ is the total crack length. Two kinds of crack were considered: cracks with uniform serration geometry and cracks with varying tooth geometry along the front. The regions with different tooth geometry are defined by the length parameters $L_A$, $L_B$ and $L_C$ in Fig. 6; the serration geometry in these regions approximates the real crack front roughness experimentally observed in the regions A, B and C of Fig. 2, as shown by the comparison between modeled and experimental cracks in Fig. 6. The mode II Stress Intensity Factor (SIF) $K_{II}$ was calculated at the left crack tip by linear regression of the relative shear displacement field along the crack front very close to the tip.

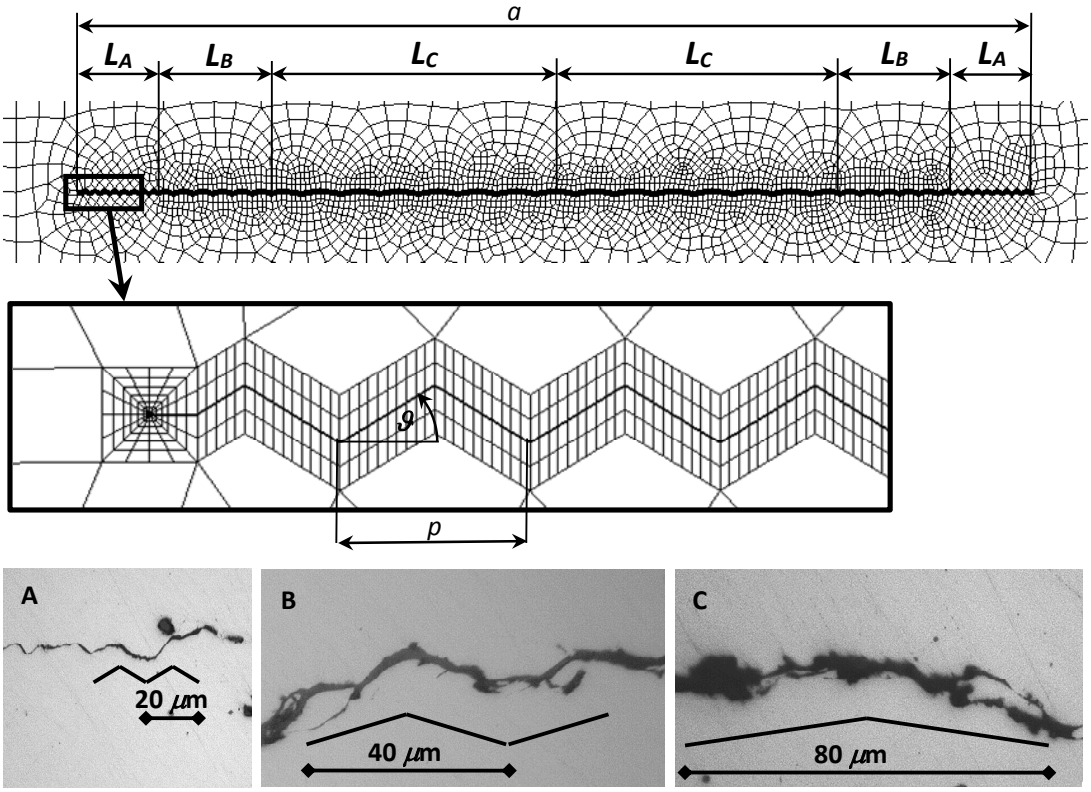


Fig. 6. FEM model of the crack front and comparison with experimental crack front geometry

Fig. 7a shows the results relative to cracks with uniform tooth geometry along the crack front, where the pitch has constant value $p$ = 20 $\mu$m and the tooth flank slope varies from $\vartheta$ = 0° (flat crack) to $\vartheta$ = 45° (very rough crack). The effect of roughness severity on the mode II SIF variation $\Delta K_{II}$ during a load pass for varying crack length is shown. The serration geometry strongly influences the applied $\Delta K_{II}$: in particular, for very rough surfaces there is a severe

closure effect, keeping the applied $\Delta K_{II}$ almost constant despite the crack length increment. This is in agreement with the cited results of Matsunaga et al. [11], who found that the mode II propagation threshold is significantly higher for cracks with rough and interfering faces, due to the locking effect of asperities. The curves can be interpolated by a power law, whose exponent is approximately 0.5 for flat cracks and tends to 0 as far as the crack front roughness increases.

Fig. 7b shows the results relative to varying tooth geometry along the crack front. In particular, the curve indicated as "rough" refers to a crack whose tooth slope $\vartheta$ is progressively reduced in the central region as far as the crack grows; the "defect" curve refers to a crack emanating from a defect, assumed as a flat crack as long as the maximum expected inherent defect for the ring specimens under investigation, i.e. 170 $\mu$m [6]. Even for the case of a crack emanating from a defect the front is progressively smoothed by wear in the central region during growth. Table 1 gives the variation of the geometric parameters in the different phases of the propagation. The "rough" curve is overlapped to the curve of uniform serration with $\vartheta = 30°$ up to 330 $\mu$m; after that, $\Delta K_{II}$ begins to increase more rapidly due to the appearance of smoother central regions. The "rough" curve is significantly lower than the curve referring to a uniform serration with slope $\vartheta = 11°$, that is comparable to that of the central region ($\vartheta = 9°$), even when this region is very long. In presence of the central flat zone ("defect") the curve starts from the expected $\Delta K_{II}$ for a smooth crack, but as far as the rough region increases, the curve rapidly tends to overlap the "rough" curve. These results show that the roughness of the central crack front region is not determinant in crack propagation, as the applied SIF mainly is influenced by the roughness close to the tip.

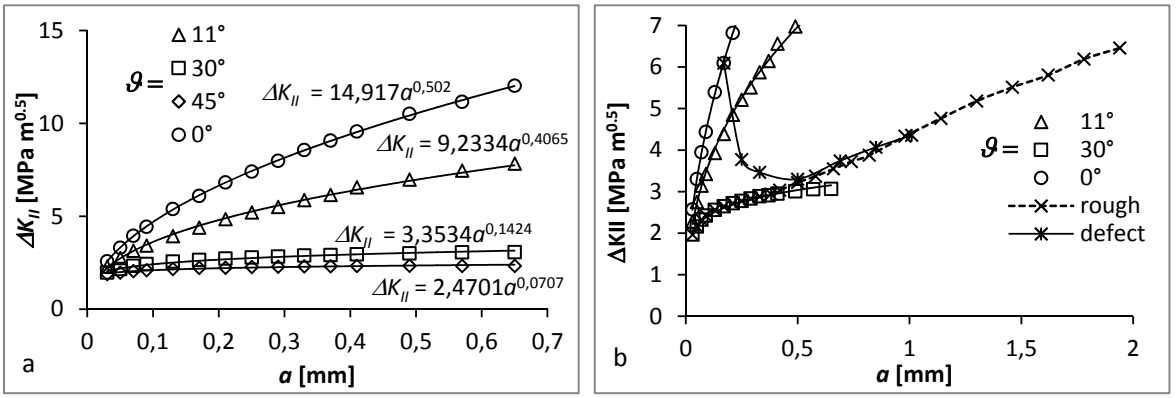


Fig. 7. (a) crack growth with uniform serration geometry; (b) crack growth with non-uniform and uniform serration geometry.

Table 1. Geometric parameters during the growth of cracks with non-uniform roughness.

| | Rough crack | | | Crack emanating from defect | |
|---|---|---|---|---|---|
| | Phase 1 | Phase 2 | Phase 3 | Phase 1 | Phase 2 |
| Total crack size $a$ [mm] | 0.03 – 0.33 | 0.33 – 0.82 | 0.82 – 1.94 | 0.17 – 0.5 | 0.5 – 1.01 |
| Length of maximum roughness portion $L_A$ [mm] | 0.015 – 0.165 | 0.165 | 0.165 | 0 – 0.165 | 0.165 |
| Length of intermediate roughness portion $L_B$ [mm] | 0 | 0 – 0.245 | 0.245 | 0 | 0 – 0.255 |
| Length of minimum roughness portion $L_C$ [mm] | 0 | 0 | 0 – 0.56 | 0.17 | 0.17 |
| Maximum roughness tooth pitch $p_A$ [mm] | | 0.02 | | | 0.02 |
| Intermediate roughness tooth pitch $p_B$ [mm] | | 0.04 | | | 0.04 |
| Minimum roughness tooth pitch $p_C$ [mm] | | 0.08 | | | 0.17 |
| Maximum roughness tooth slope $\vartheta_A$ [°] | | ~31 | | | ~31 |
| Intermediate roughness tooth slope $\vartheta_B$ [°] | | ~17 | | | ~17 |
| Minimum roughness tooth slope $\vartheta_C$ [°] | | ~9 | | | 0 |

This curve also shows that even if an inherent crack is able to propagate because the applied $\Delta K_{II}$ exceeds the propagation threshold $\Delta K_{IIth}$, the "zigzag" propagation mechanism will rapidly lower the applied $\Delta K_{II}$, maybe underneath the propagation threshold. Therefore, wear between crack faces plays a very important role in propagation, as it reduces the crack front roughness re-approaching the applied $\Delta K_{II}$ to the propagation threshold. Crack growth is expected to proceed by subsequent propagation-arrest-wear steps across the threshold $\Delta K_{IIth}$, until the crack dimension is large enough to allow propagation even with severe roughness near the tip, as is qualitatively shown in Fig. 8.

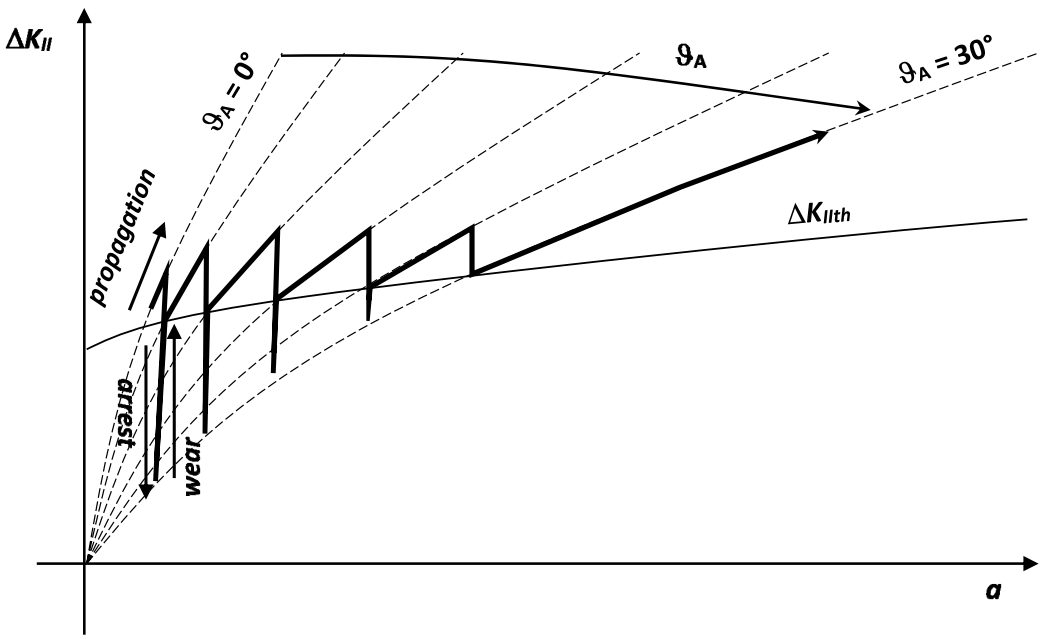


Fig. 8. Qualitative crack growth behavior of a rough crack.

## 4. Conclusions

The experimental results of Rolling Contact Fatigue tests on a gear steel were examined in order to study the mechanism of subsurface crack propagation, leading to spalling. A subsurface crack front and its fracture surface were analyzed by means of Scanning Electron Microscopy. The crack front had a serrated shape, varying along the crack length. Micro-particles de-attaching from the crack faces were observed, acting as third body between the crack faces. These particles were furtherly fragmented in a very fine powder: this phenomenon, due to the combined effect of compressive and shear stresses, can be recognized as wear. It was more significant in the central crack zone, where a gap between the crack faces was formed and the severity of the crack front serration was reduced.

A finite simulation of this mechanism was carried out, taking into account the serrated crack front shape and the reduction of crack faces roughness in the central region due to wear. The simulation results showed that the crack front roughness plays a very important role in reducing the applied mode II stress intensity factor, by means of the shear locking effect due to asperities. This effect is mainly determined by the roughness of the region close to the crack tip, even when a long smooth central region is present. Cracks emanating from inherent defects can arrest after a propagation step due to the locking effect due to roughness, but wear can progressively reduce the crack front

roughness allowing further propagation. A mechanism of stepped growth across the propagation threshold was hypothesized for short cracks.

These results show that the experimental determination of the propagation thresholds in mode II and mode III should take into account the shear locking effect, in order to depurate it from the effect related to material properties, as confirmed by the experimental results of Matsunaga et al. [11].

## References

[1] R.S. Hyde, Contact fatigue of hardened steel. ASM Handbook. 19 (1996) 691–703.
[2] R. Pedersen, S.L. Rice, Case crushing of carburized and hardened gears. SAE Trans. 68 (1960) 187-200.
[3] D. Nélias, M.L. Dumont, F. Champiot, A. Vincent, D. Girodin, R. Fougères et al., Role of inclusions, Surface Roughness and Operating Conditions on Rolling Contact Fatigue. J of Tribology. 121 (1999) 240-251.
[4] E. Bormetti, G. Donzella, A. Mazzù, Surface and subsurface cracks in rolling contact fatigue of hardened components, Tribology Trans, 45 N3 (2002) 274-283.
[5] M.W.J. Lewis, B. Tomkins, A fracture mechanics interpretation of rolling bearing fatigue, Proc Instn Mech Engrs Part J: Journal of Engineering Tribology. 226 (2012) 389-405.
[6] G. Donzella, M. Faccoli, A. Mazzù, C. Petrogalli, H. Desimone, Influence of inclusion content on rolling contact fatigue in a gear steel: experimental analysis and predictive modeling. Engng Fract Mech. 78 (2011) 2761–2774.
[7] W.W. Cheng, H.S. Cheng, Semi-analytical modeling of crack initiation dominant contact fatigue life for roller bearings. J Tribol. 119 (1997) 233–40.
[8] A.P. Voskamp, Fatigue and Material Response in Rolling Contact. Bear Steel: Into the 21st Century, ASTM. 1327 (1998) 152-166.
[9] B. Lv, M. Zhang, F.C. Zhang, C.L. Zheng, X.Y. Feng, L.H. Qjan, X.B. Qin, Micro-mechanism of rolling contact fatigue in Hadfield steel crossing, International Journal of Fatigue. 44 (2012) 273-278.
[10] A. Otsuka, Y. Fujii, K. Maeda, A new testing method to obtain mode II fatigue crack growth characteristics of hard materials, Fatigue Fract Engng Mater Struct. 27 (2004) 203-212.
[11] H. Matsunaga, N. Shomura, S. Muramoto, M. Endo, Shear mode threshold for a small fatigue crack in a bearing steel, FFEMS, 34 (2010) 72-82.
[12] S. Beretta, S. Foletti, K. Valiullin, Fatigue crack propagation and threshold for shallow micro-cracks under out-of-phase multiaxial loading in a gear steel. Eng Fract Mech. 77 (2010) 1835-1848.